

## Photodisintegration of the Deuteron at 20 Mev\*

J. HALPERN AND E. V. WEINSTOCK  
*University of Pennsylvania, Philadelphia, Pennsylvania*  
 (Received May 19, 1953)

Counter techniques have been applied to a study of the proton angular distribution in the photodisintegration of the deuteron induced by bremsstrahlung photons from a betatron in the energy interval 18–22 Mev. The measured distribution is given by  $A + \sin^2\theta(1 + 2\beta \cos\theta)$ , with  $A = 0.132 \pm 0.041$  and  $\beta \cong 0.1$ . The total cross section is also measured.

### INTRODUCTION

THE photodisintegration of the deuteron at low energies has now been exhaustively studied,<sup>1</sup> and the agreement between theory and experiment is excellent. The process, on the other hand, is independent of the shape of the neutron-proton interaction and yields no new information other than verify the application of the effective range concept to the photodisintegration experiments.<sup>2</sup>

At intermediate energies (in the region where relativistic effects are still small and free meson effects are not involved), accurate measurements of total cross section and angular distribution are sensitive to the details of the force law as regards shape of the potential, the percentage of charge exchange, and the nature of the tensor forces assumed. During the past few years several theoretical treatments of the problem have appeared, the salient results of which follow.

In the energy region from 10 to 100 Mev, the photoelectric dipole transition from the  $^3S_1$  ground state to

$^3P_{0,1,2}$  states is the dominant transition. Using central forces only, Schiff<sup>3</sup> and Marshall and Guth<sup>4</sup> have shown that the Yukawa and exponential potentials yield about the same dipole cross section, though there is a pronounced dependence on the effective range and the percentage of exchange. The angular distribution has the form of  $\sin^2\theta$ . The electric quadrupole transition  $^3S \rightarrow ^3D$ , although not materially affecting the cross section, does alter the angular distribution by interference with the  $^3P$  waves to produce a fore-aft asymmetry given by  $\sin^2\theta(1 + 2\beta \cos\theta)$ , where  $\beta = [(h\nu - \epsilon)/Mc^2]^{\frac{1}{2}}$ ,  $h\nu$  = photon energy,  $\epsilon$  = deuteron binding energy, and  $M$  = mass of proton or neutron. Austern,<sup>5</sup> in calculating the effects produced by the inclusion of noncentral interactions, has shown that again the total cross section is not much affected, but an isotropic term is introduced into the angular distribution arising through the  $D$ -wave admixture in the deuteron ground state, but principally through the removal of the degeneracy in the  $^3P_j$  states in the outgoing waves. Thus an odd-

TABLE I. Summary of previous measurements.

Authors	Mean $\gamma$ energy (Mev)	$\gamma$ 's produced by	Target and detector	$\sigma \times 10^{28}$ cm <sup>2</sup>	A
Hough	6.13 (6.1 and 7)	(F + $p$ )	Emulsions	—	0.02 <sup>+0.04</sup> —0.02
	17.6 (14.8 and 17.6)	(Li + $p$ )	Deuterium-loaded paraffin target	7.2 ± 1.5	0.02 <sup>+0.14</sup> —0.02
Wilkinson and Carver	4.45	N <sup>15</sup>	Deuterium-filled ion chamber	24.3 ± 1.7	
	6.14	F <sup>19</sup>		21.9 ± 1.0	
	7.39	Be <sup>9</sup>		18.4 ± 1.5	
	8.14	C <sup>13</sup>		16.4 ± 1.2	
	12.5	B <sup>11</sup>		10.4 ± 1.0	
Fuller	17.6	Li <sup>7</sup>		7.7 ± 0.9	
	13.3	Bremsstrahlung from betatron	Deuterium gas and photographic emulsions		~0.05 ~0.2
Waffler and Younis	14.8 and 17.6	Li <sup>7</sup> + $p$	Loaded emulsions	7.1 ± 1.5	0.12 ± 0.07
G. Goldhaber	6.1 and 7	F <sup>19</sup> + $p$	Loaded emulsions		0.15 ± 0.06
Phillips, Lawson, and Kruger	6.14 and 7	(F + $p$ )	Cloud chamber	25.7 ± 14%	
Krohn and Shrader	11–13	Betatron	Loaded emulsions		0.24 ± 0.07
	6–8	bremsstrahlung			0.05 ± 0.05
Gibson, Grottdal, Orlin, and Trumpy	6.13 and 7	(F + $p$ )	Loaded emulsions		~0

\* Supported in part by the Air Research and Development Command and the joint program of the U. S. Office of Naval Research and the U. S. Atomic Energy Commission.

<sup>1</sup> Bishop, Collie, Halban, Hedgran, Siegbahn, du Toit, and Wilson, Phys. Rev. **80**, 211 (1950); Bishop, Halban, Shaw, and Wilson, Phys. Rev. **81**, 219 (1951).

<sup>2</sup> H. A. Bethe and C. Longmire, Phys. Rev. **77**, 647 (1950).

<sup>3</sup> L. I. Schiff, Phys. Rev. **78**, 733 (1950).

<sup>4</sup> J. F. Marshall and E. Guth, Phys. Rev. **78**, 738 (1950).

<sup>5</sup> N. Austern, Phys. Rev. **85**, 283 (1952).

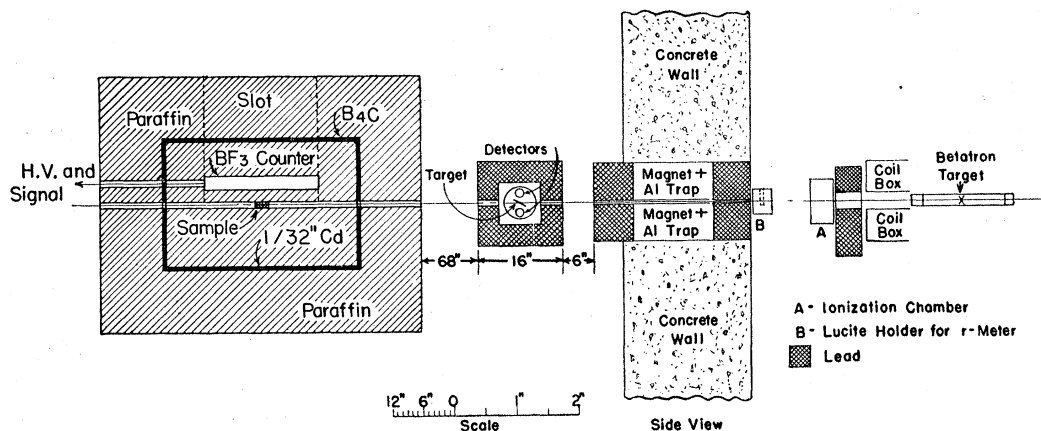


Fig. 1. General arrangement of apparatus showing beam collimator, proton detection assembly, and neutron monitor.

state noncentral interaction will affect the deuteron photodisintegration, though it has no strong influence on  $n$ - $p$  scattering data.<sup>6</sup> The total angular distribution becomes  $A + \sin^2\theta(1 + 2\beta \cos\theta)$ . There will be a contribution to  $A$  arising from any vestige of the photomagnetic cross section remaining at the energies being considered.

Measurements of the cross section and angular distribution in the region up to 20 Mev have recently been made in several laboratories,<sup>7-14</sup> and the results are summarized in Table I. Although the total cross-section measurements show errors of the order of ten percent as a result of the small cross section for the reaction and the inherent difficulty in determining photon fluxes, the expected energy dependence is found and the results rule out a potential based on pure ordinary forces without exchange. The determination of the percentage of exchange in the central force requires greater accuracy.

In the angular distribution measurements summarized in Table I, most observations have demonstrated the dipole-quadrupole interference term, and the percentage of quadrupole interaction is in general accord with predictions. The isotropic term, however, remains in doubt. The general trend of the values seems considerably higher than can be explained along the lines of the theoretical treatment of Austern.

All the angular distribution measurements in this energy region have been made using photographic emulsions as detectors for the photoprotons, and inadequate statistics have been the limiting factor.

<sup>6</sup> R. S. Christian and E. W. Hart, Phys. Rev. **77**, 441 (1950); K. M. Case and A. Pais, Phys. Rev. **80**, 203 (1950).

<sup>7</sup> P. V. C. Hough, Phys. Rev. **80**, 1069 (1950).

<sup>8</sup> J. H. Carver and D. H. Wilkinson, Nature **167**, 154 (1951).

<sup>9</sup> E. G. Fuller, Phys. Rev. **79**, 303 (1950).

<sup>10</sup> H. Wäffler and S. Younis, Helv. Phys. Acta **24**, 483 (1951).

<sup>11</sup> G. Goldhaber, Phys. Rev. **81**, 930 (1951).

<sup>12</sup> Phillips, Lawson, and Kruger, Phys. Rev. **80**, 326 (1950).

<sup>13</sup> V. E. Krohn, Jr. and E. F. Shrader, Phys. Rev. **86**, 391 (1952).

<sup>14</sup> Gibson, Grottdal, Orlin, and Trumpy, Phil. Mag. **42**, 555 (1951).

Using ZnS detectors previously employed for studying photoprotons from other elements,<sup>15</sup> we have applied counter techniques to the angular distribution in the  $D(\gamma, p)n$  reaction induced by bremsstrahlung photons from a betatron in the energy interval 18–22 Mev in order to establish with greater certainty the value of the isotropic component. The total cross section is also obtained. The prior experience with the apparatus in determining proton angular distributions from elements with relatively high yields gave added confidence in its use with deuterium.

#### APPARATUS AND PROCEDURE

The apparatus, described in detail elsewhere,<sup>15,16</sup> is shown in Fig. 1. Briefly, a strongly collimated bremsstrahlung beam of maximum energy 22 Mev strikes a 25-mg/cm<sup>2</sup> deuterated paraffin target placed at a given angle (60 degrees) with respect to two identical ZnS scintillators diametrically opposite each other. The detectors subtend an angle of  $\pm 5$  degrees at the target. Between the target and detectors, and adjacent to the latter, are placed aluminum proton absorbers the details of which will be described below. The target and detectors rotate as a unit about the incident beam direction, the relative orientation of target and detectors remaining fixed throughout the experiment. After passing through the deuterated paraffin target, the bremsstrahlung beam strikes a 2-g/cm<sup>2</sup> tantalum target contained in a neutron detection assembly, and the number of neutrons from the  $Ta(\gamma, n)$  reaction is used to monitor the bremsstrahlung intensity.

The purpose of the aluminum foils between target and detector is to remove all protons produced by photons of energies less than 18 Mev, so that the effects observed are the result of a narrow band of photons in the 18–22-Mev interval of the bremsstrahlung. Because of the high carbon ( $\gamma, p$ ) threshold (18 Mev), no protons

<sup>15</sup> Mann, Halpern, and Rothman, Phys. Rev. **87**, 146 (1952); A. K. Mann and J. Halpern, Phys. Rev. **82**, 733 (1951).

<sup>16</sup> Halpern, Mann, and Nathans, Rev. Sci. Instr. **23**, 678 (1952).

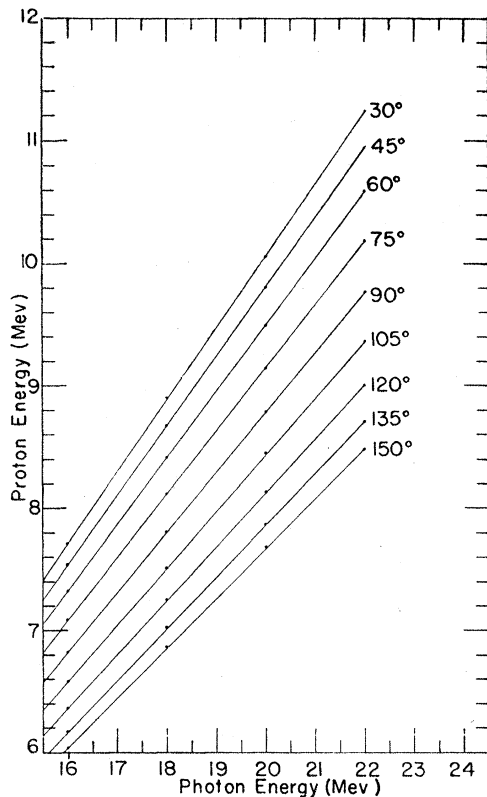


FIG. 2. Curves showing effect of center-of-mass correction on laboratory proton energies at different angles.

reach the detector as a result of the carbon in the deuterated paraffin target. The proton energy corresponding to a photon of 18 Mev changes drastically with angle due to the center-of-mass correction (Fig. 2), ranging in energy from 8.90 Mev at  $30^\circ$  to 6.86 Mev at  $150^\circ$ . As a result, absorber thicknesses vary with angle.

Measurements were made simultaneously with the two identical ZnS detectors, each covering the region from 30 to 330 degrees. Data could not be taken in the intervals from 150 to 210 and from 330 to 30 degrees because in these regions the beam would strike the detector assembly. Outputs from the detectors were fed through cathode followers into model 100 amplifiers and then into ten-channel integral pulse-height selectors. At each angular setting, integral bias curves were taken with a deuterated paraffin and then with a normal paraffin target of equivalent thickness to determine the background. After normalization to equal yield of neutrons from the beam monitor, background curves were then subtracted from those taken with the deuterated target as illustrated in Fig. 3 for one of the  $90^\circ$  runs. The resultant curves were then extrapolated to zero bias for the final readings. The betatron was operated at the same output level for deuterated target and blank to insure that background arising from

cosmic rays and any light particle pileup would be canceled out completely. The useful counting rate at  $90^\circ$  was 0.6 count per minute, and data collection for six months yielded approximately 10 000 useful counts at all angles. Two separate deuterated paraffin targets were used, and results were compared.

## CORRECTIONS AND ERRORS

### (a) Finite Thickness of Target

Since the relative orientation of target and detectors remains fixed as the angle of detection of photoprotons is varied, differential proton absorption in the target should be the same for all angles. This would be strictly so were it not for the change in proton energy in the laboratory system with angle and the resultant change in proton energy loss in the target. The aluminum foils between target and detector were so chosen that at a given angle a proton leaving the center of the target would not reach the detector unless produced by a photon of energy exceeding 18 Mev. Protons reaching the detector from the front half of the target would

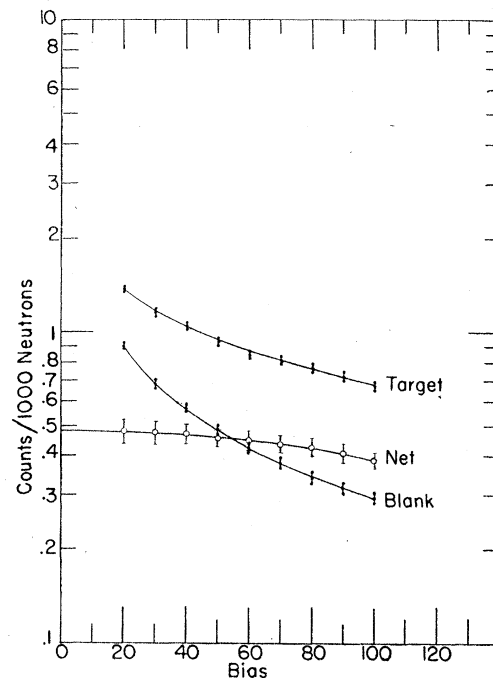


FIG. 3. Integral bias curves for the ZnS detectors taken with deuterated paraffin target and with normal paraffin target for the  $90^\circ$  angle. The difference curve is then extrapolated to zero bias to determine counting rate.

contain a portion produced by lower-energy protons; and conversely some of the protons produced by photons exceeding 18 Mev would be absorbed if originating from the back half of the target. Figure 4 illustrates the effect quantitatively for the two extreme angles of  $30^\circ$  and  $150^\circ$ . The area under the solid curve of the figure represents the relative number of protons

to be expected for an infinitely thin target. It is the product of the bremsstrahlung energy dependence (Schiff spectrum) and the photodisintegration cross-section energy dependence (Bethe-Peierls expression), cut off at 18 Mev. The two different dashed curves show how the area is modified for target absorption at the 30° and 150° angle settings. For each angle, the added protons from the front half of the target almost compensate the loss of protons from the back half. Figure 5 gives the calculated correction factor as a function of angle. Since this correction factor never exceeds 3 percent, application to the data should eliminate target thickness affects to the order of 1 percent.

### (b) Geometric Factors

Since the target changes its orientation with respect to the x-ray beam as the detection angle is varied, the

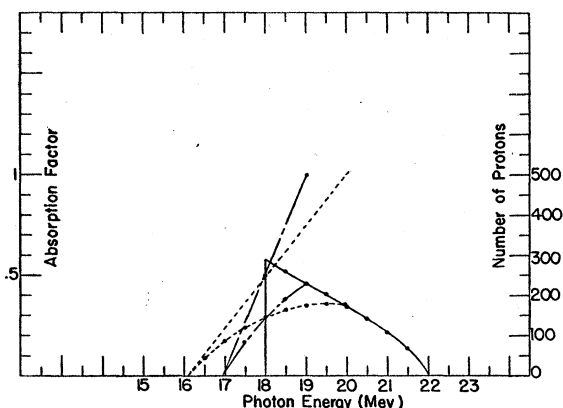


FIG. 4. Curves illustrating effect of finite target thickness. The straight lines represent fraction of protons absorbed in target at a given energy.

effective target thickness varies with angle. To normalize the data to the same effective target thickness with the degree of precision necessary and to assure that the center of the x-ray beam passed through the axis of rotation of the rotating unit, optical and photographic methods were used in the manner described in reference 15. Angles between beam and target were known to  $\pm 0.5$  degree, and angles between beam and detectors to  $\pm 2$  degrees.

As the angle between target and incident beam is varied, the source of photoprotons changes shape from a circle of diameter 7 mm (when the target surface is perpendicular to the beam direction) to an ellipse of eccentricity two (when angle between target surface and beam is 30 degrees). This produces only second-order changes in the solid angle but requires that the target be uniform in thickness over a 14-mm diameter. The experiment was performed using two targets prepared from deuterated wax obtained from different producers and results were the same within statistical uncertainties. The 30-degree and 150-degree data were

taken with the target perpendicular to the beam and repeated with the target 30 degrees to the beam. After target thickness normalization, the results again agreed.

The finite angle subtended by the detectors will introduce an added symmetric term in any angular correlation measurement, the correction increasing as the detector angular size increases. Since this is a constant term, its importance depends on the observed percentage of symmetric component in the angular distribution. Using the method of Frankel,<sup>17</sup> we have calculated this effect and find that it amounts to only 2 percent of the measured symmetric component for the geometry of this experiment. Similarly, scattering in the aluminum absorbers can be neglected especially since they have been placed as close to the ZnS screens as possible to minimize the effect.

To convert all data into center-of-mass system, correction must be made for change of center-of-mass solid angle with setting of detector. This correction amounts to approximately  $\pm 12$  percent over the angles of detection employed. Similarly, conversion of laboratory angles to center-of-mass angles results in a maximum angular shift of approximately 3 degrees.

### (c) Energy Control

Reference to Fig. 4 shows that the photoproton yield is sensitive to the maximum bremsstrahlung energy, which must be maintained constant throughout the experiment. Energy instability in operation of the betatron will be reflected in an instability in the useful photon flux. The betatron energy can be maintained to an accuracy of  $\pm 0.1$  Mev over long time intervals, as was indicated by periodic checks of the energy scale through measurement of photoneutron threshold of bismuth during the course of the experiment. Errors arising from energy fluctuations are to a large extent compensated by the use of the Ta( $\gamma, n$ ) beam monitor, for as the maximum bremsstrahlung energy increases, the ( $\gamma, n$ ) yield from the monitor also increases and the photoproton yield from the deuterated paraffin remains essentially constant when normalized to a given number

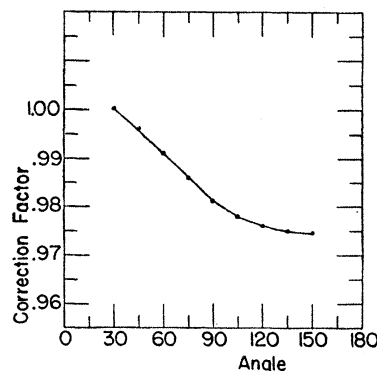


FIG. 5. Target absorption multiplying factors for different angles computed from data taken from Fig. 4.

<sup>17</sup> Sherman Frankel, Phys. Rev. 83, 673 (1951).

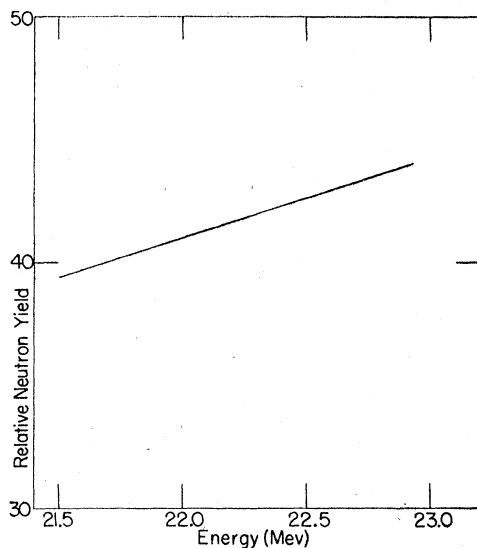


Fig. 6. Energy response of Ta( $\gamma,n$ ) beam monitor.

of neutrons from the monitor. Figure 6 shows the monitor yield in neutrons per roentgen as a function of betatron energy, the betatron beam being also monitored by an ionization chamber and current integrator calibrated in roentgen. To test the compensation against energy fluctuations, the  $90^\circ$  proton yield per neutron was measured for a betatron energy of 22 Mev and 22.2 Mev, and variations were within the error of the experiment. Despite this, no data were used in which the monitor neutron yield per roentgen showed appreciable deviations from the statistical average.

#### (d) Errors Affecting Total Cross Section

For the determination of the value of the total cross section for the reaction, several additional uncertainties (that do not influence the angular distribution results) become important. The most serious of these is the

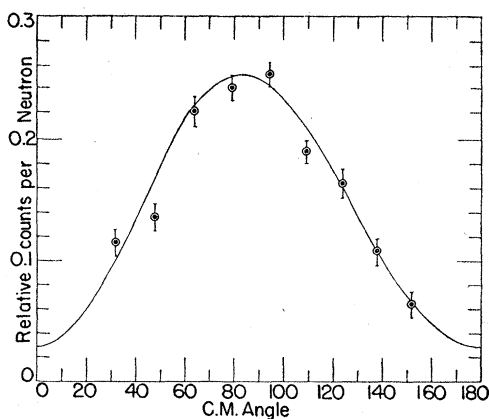


Fig. 7. Angular distribution of photoprotons observed. Errors attached to the experimental points are the statistical uncertainties.

uncertainty in the determination of the exact number of photons in the portion of the bremsstrahlung used. This measurement involves the conversion of the response of an R thimble imbedded in Lucite into energy units to compute the total photon intensity in the betatron beam,<sup>18</sup> and then involves the detailed shape of the bremsstrahlung distribution to calculate that portion of the beam in the energy interval between 18 and 22 Mev.<sup>19</sup> Without better measurements of the energy content of the beam, it would be difficult to estimate the photon intensity to better than 20 percent. Future contemplated calibrations with a pair spectrometer should, however, improve the quoted total cross-section value.

An additional uncertainty arises from the assumption that the ZnS screens have an efficiency of 100 percent for the detection of low-energy protons. From comparison of photoproton yields, measured in other elements, using the ZnS detectors with data taken using photographic plates and radioactive techniques, the

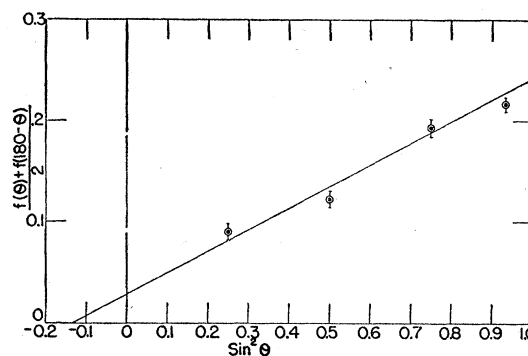


Fig. 8. Angular distribution folded about  $90^\circ$ . Intercept with  $\sin^2 \theta$  axis gives value of symmetric component in angular distribution.

efficiency of the detectors is believed to be 100 percent to within an accuracy of 5 percent.

Other uncertainties, such as number of deuterium atoms in the target and exact solid angle subtended by the detectors, should be negligibly small compared with the above.

#### RESULTS AND DISCUSSION

Some five thousand useful counts were recorded at all angles from the two detectors in one experiment, and then the runs were repeated using a second deuterated paraffin target for a total of ten thousand counts. Figure 7 shows the resulting angular distribution observed by combining the results from both targets and both detectors. The data at  $90^\circ$  taken with the individual detectors agreed within 5 percent, while the two separate runs with different targets agreed within 3 percent.

<sup>18</sup> Johns, Katz, Douglas, and Haslam, Phys. Rev. **80**, 1062 (1950).

<sup>19</sup> L. I. Schiff, Phys. Rev. **70**, 87 (1946); **83**, 252 (1951).

The curve drawn through the experimental points in Fig. 7 has the form

$$f(\theta) = A + \sin^2\theta(1 + 2\beta \cos\theta),$$

with  $A = 0.132 \pm 0.041$  and  $\beta = 0.1$ . Fitting the above parameters to the data was done in the usual manner of folding the observed angular readings about  $90^\circ$  as illustrated in Fig. 8, in which

$$\phi(\theta) = \frac{1}{2}[f(\theta) + f(180^\circ - \theta)] = A + \sin^2\theta$$

is plotted against  $\sin^2\theta$ . The resulting points should fall on a straight line whose intercept with the  $\sin^2\theta$  axis gives the value of  $A$  independent of the value of  $\beta$ . The straight line drawn through the data of the figure is determined by the method of least squares. The observed value for  $A$  is consistent, for the most part, with previous observations of less accuracy at slightly reduced energies.

Similarly,  $\beta$  can be determined independent of the assumed value for  $A$  by plotting  $f(\theta) - f(180^\circ - \theta)$  against  $\sin^2\theta \cos\theta$ . The determination of  $\beta$  is subject to

considerably greater statistical uncertainty. Its order of magnitude does, however, agree well with what should be expected at these energies and represents an additional check on the experiment.

Integration of the angular distribution leads to a value of the total cross section,

$$\sigma = 5.4 \times 10^{-28} \text{ cm}^2.$$

The uncertainty in the total cross section is large, and its agreement with the calculated value of Marshall and Guth for 50 percent exchange ( $5.5 \times 10^{-28} \text{ cm}^2$ ) is fortuitous.

The size of the "isotropic" term  $A$  in the measured angular distribution can arise only from the noncentral part of the neutron-proton interaction. Austern has attempted to estimate the quantitative effects resulting from the noncentral potential on the isotropic term and has shown that the results are sensitive to both the shape and percent of exchange in the tensor term. The calculations are not of sufficient accuracy to permit further conclusions at this time.

### The Excitation Function for the $\text{Al}^{27}(d, \alpha p)\text{Na}^{24}$ Reaction\*

R. E. BATZEL, W. W. T. CRANE, AND G. D. O'KELLEY  
*California Research and Development Company, Livermore, California*  
 (Received May 18, 1953)

The absolute cross section for the  $\text{Al}^{27}(d, \alpha p)\text{Na}^{24}$  ( $T_{1/2} = 15.1$  hr) reaction has been measured as a function of deuteron energy from the threshold to 190 Mev. Targets were irradiated on the Berkeley 60-inch and 184-inch cyclotrons. The observed threshold is  $11.0 \pm 0.5$  Mev; and the excitation function has a pronounced peak of 53 millibarns at approximately 22 Mev, falls to a broad minimum of 18 millibarns in the region of 60 Mev, and then rises slowly to 22 millibarns at 190 Mev.

#### INTRODUCTION

THE excitation function for the  $\text{Al}^{27}(d, \alpha p)\text{Na}^{24}$  reaction has been measured as a function of deuteron energy from the threshold to 190 Mev by the stacked foil technique. The absolute cross section for the reaction as a function of energy is of particular interest since the  $\text{Na}^{24}$  induced in aluminum foils irradiated concurrently with targets in the internal circulating beam of the Berkeley 184-inch frequency-modulated cyclotron can be used to monitor the deuteron beam where direct measurement is not possible.  $\text{Na}^{24}$  has a convenient half-life (15.1 hours)<sup>1</sup> for counting and is the principal activity produced by high energy deuteron bombardment of aluminum.  $\text{F}^{18}$  ( $T_{1/2} = 112$  min) is the major interfering nuclide,<sup>2</sup> and this activity has decayed sufficiently 8 to 10 hours after bombardment that it is no longer detectable.

The excitation function has been measured previously for the energy region of interest,<sup>3</sup> but in these experiments no attempt was made to correct for losses of beam due to multiple Coulomb scattering and nuclear absorption, and errors due to loss of  $\text{Na}^{24}$  by recoil or  $\text{Na}^{24}$  induced by stripped and high-energy neutrons formed in the process of degrading the deuteron energy by the use of copper absorbers.

The absolute cross section of the  $\text{Al}^{27}(d, \alpha p)\text{Na}^{24}$  reaction has previously been measured for 190-Mev deuterons;<sup>4</sup> but in view of the importance of the absolute value for the cross section, this measurement was repeated.

#### PROCEDURE

##### Irradiations

Targets for the Berkeley 184-inch cyclotron were irradiated in the internal circulating beam and in the

\* This work was done under the auspices of the U. S. Atomic Energy Commission.

<sup>1</sup> J. H. Sreb, Phys. Rev. **81**, 469 (1951).

<sup>2</sup> F. O. Bartell and S. Softky, Phys. Rev. **84**, (1951).

<sup>3</sup> W. W. Meinke, Ph.D. thesis, University of California, (unpublished).

<sup>4</sup> H. Hubbard, Phys. Rev. **75**, 1470 (1949).